JOURNAL OF MATERIALS SCIENCE 23 (1988) 894–899

Oxidation and decarburization of an Fe–Al–C alloy

C. H. KAO, C.M. WAN
Institute of Materials Science and Engineering, National Tsing Hua University, Hsinchu, Taiwan

The oxidation behaviour of the Fe–5.5Al–0.55C (wt%) alloy was studied in air at 500 to 950° C. Specimens of two types of preparation were used: (i) homogenized for 4 h at 1100° C under an argon protective atmosphere to form carbide particles in the ferrite matrix (referred to Type 1 alloy); and (ii) homogenized for 96 h at 1100° C under an air atmosphere to form a ferrite matrix with full decarburization (Type 2 alloy). Type 1 alloy with or without a decarburized zone after oxidation had a higher oxidation rate than Type 2 alloy. The oxidation kinetics of Type 1 alloy are controlled by the stability of carbide particles. The interference of CO or CO_2 formation influences vitally the formation of protective aluminium oxide. During the oxidation of Type 2 alloy, two oxidation periods appear with slightly different parabolic constant values. The oxidation rate increased with temperature to a maximum at 600° C and then decreased to a minimum at 800° C.

1. Introduction

Our recent work [1] concludes that the kinetic behaviours of Fe–5.5Al–0.55C (wt%) alloy at 600, 800 and 1000° C are drastically influenced by the stability of carbide in the matrix. At 600 °C, a simple parabolic law was observed. There are three distinct parabolic rates and two distinct parabolic rates for the alloy at 800 and 1000° C, respectively. The carbon atoms which come from the dissociation of carbide particles play a most important role in the kinetic behaviour. To be sure, a change of the diffusion rate of carbon with changing oxidation temperature is another important factor in the oxidation behaviour of the present alloy. However, the temperatures used in the previous work [1] were too few to fully understand the oxidation behaviour of the alloy. Therefore, the oxidation temperatures used in the present experiment ranged from 500 to 950° C and were increased in increments of 50° C. In addition, in order to understand thoroughly the effect of decarburization on the oxidation behaviour of the Fe–5.5Al–0.55C alloy, heat treatment was carried out on the alloy to obtain specimens with full decarburization. The specimens were then used to study the oxidation process at oxidation temperatures from 500 to 900° C. The results of this investigation are expected to interpret the relationship between oxidation and decarburization of the Fe–Al–C alloy.

2. Experimental procedure

The chemical composition of the alloy used for the present study is shown in Table I. The alloy was prepared with an air induction furnace under a controlled protective argon atmosphere. The cast ingot was hot-forged at 1200° C from 7 cm to 2.5 cm. The alloy was heat-treated as follows: (i) homogenized for 4 h at 1100° C with a tube furnace under an argon protective atmosphere (Type 1 alloy); or (ii) homogenized for 96 h at 1100° C with the same furnace under a dry air atmosphere (Type 2 alloy). After surface finishing the surfaces and edges of the specimens were mechanically polished with abrasive paper up to 1200 grit. Finally each specimen was cleaned ultrasonically in acetone before the oxidation experiments.

The kinetics of oxidation were measured in the infrared image furnace of an Ulvac/Shink–Uriko thermobalance in dry air with a flow rate of 100 ml min^{-1}. The isothermal oxidation period was 24 h and the heating and cooling rates were 100° C min^{-1}. The specimen temperature and weight gain curves of oxidation were recorded with a chart recorder.

After oxidation, samples were mounted and examined by optical microscopy. The possible phases present in different specimens were identified with X-ray diffraction using a copper target, a nickel filter and a graphite single-crystal monochromator. The elemental distributions and concentration profiles in the oxidized specimens were characterized by electron microanalysis (EPMA) (Jeol JCXA-733). EPMA was operated by first raising the voltage to 25 kV with a probe current of 0.03 μA.

3. Results and discussion

From the previous report [1], Type 1 alloy (Fe–5.5Al–0.55C alloy after hot forging and 4 h homogenization at 1100° C under an argon protective atmosphere) was found to be a two-phase material with iron–aluminium carbide (Fe_3AlC_x) in the ferrite matrix. Type 2 alloy (the present alloy after hot forging and 96 h homogenization at 1100° C under an air

0022–2461/88 $03.00 + .12

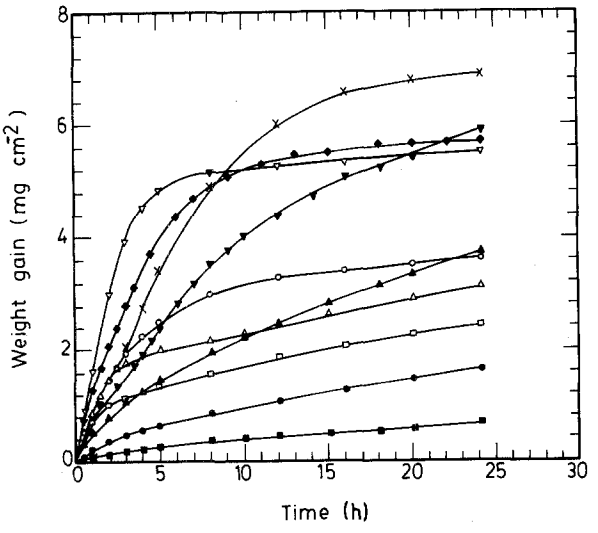

Figure 1 Thermogravimetric oxidation curves of Type 1 alloy: (■) 500° C, (●) 550° C, (▲) 600° C, (○) 650° C, (△) 700° C, (□) 750° C, (▼) 800° C, (×) 850° C, (◆) 900° C, (▽) 950° C.

atmosphere) was found to be fully decarburized in the matrix. Through optical investigation, no carbides and only a ferrite matrix could be observed in Type 2 alloy.

A plot of weight gain as a function of oxidation time and temperature for Type 1 alloy is shown in Fig. 1. Based on the square of weight gain against time curves for the present alloy, the oxidation behaviour curves can be divided into four groups. The first one, covering oxidation in the temperature range from 500 to 600° C, follows a simple parabolic rate law for up to 24 h as shown in Figs 2a, b and c. The evaluated values of the parabolic rate constant (K_p) are listed in Table II.

Using the Arrhenius equation, the oxidation rate (K_p) can be expressed as

$$K_p = (\text{constant}) \exp(-Q/RT)$$

in which Q is the activation energy (J mol^{-1}) R the gas constant (8.31 J K^{-1} mol^{-1}) and T the absolute temperature. The first group satisfies the relation in the temperature range 500 to 600° C with $K_p = 1.5 \times 10^8 \exp(-199\,700/RT)$.

The second group, covering the oxidation behaviour in the temperature range from 650 to 750° C, follows two parabolic rate laws for up to 24 h. Figs 2d, e and f show the square of weight gain per unit area against time for Type 1 alloy at 650, 700 and 750° C, respectively. The initial oxidation rate (described by the parabolic rate constant K_{pi}) was high and generally lasted for 2 to 8 h. The final oxidation rate (K_{pf}) represents the kinetics for the remainder of the experimental run and always has a low value.

Kinetic curves for the third group of oxidation curves represent the oxidation behaviour at 800 and 850° C. The square of weight gain against time for the

TABLE I Chemical composition of the Fe–Al–C alloy

Element	Al	C	Mn	Si	P	S	Fe
Composition (wt %)	5.51	0.55	0.01	0.02	0.01	0.021	Bal.

TABLE II Rate constant for oxidation between 500 and 600° C

T(° C)	K_p(g^2 cm^{-4} sec^{-1})
500	4.7×10^{-12}
550	3.2×10^{-11}
600	1.6×10^{-10}

alloy after 24 h oxidation at 800 and 850° C is shown in Figs 2g and h. The oxidation in this temperature range can be divided into three stages during 24 h. The oxidation rate of the initial stage (K_{pi}) is lower than that of the second stage (K_{pm}) and lasts for approximately 3 h. The oxidation rate (K_{pm}) of the second stage generally has the highest rate value among the three oxidation stages, which lasts about 10 to 13 h. The oxidation rate of the final stage (K_{pf}) is lower than for the second stage (K_{pm}).

Finally, the oxidation behaviours at 900 and 950° C have two parabolic rates. The first parabolic rate was found to be higher than the second one. Figs 2i and j show the square of weight gain per unit area against time for Type 1 alloy at 900 and 950° C, respectively. The parabolic rate constants of the Type 1 alloy oxidation at 650 to 950° C during 24 h were calculated and are listed in Table III. At least three specimens were used for the present study to obtain each kinetic curve. The reproducibility of each oxidation kinetic curve was approximately ± 2%.

According to optical investigations, the structures of the matrix of the Type 1 alloy after 24 h oxidation in the temperature range from 500 to 600° C are quite similar to that of the alloy before the oxidation experiment. No carbide-free layer could be observed under such conditions. However, two oxide layers which were rich in iron were evident after 24 h oxidation. These two oxide layers were similar to the oxide layer observed at 600° C. The only difference was the thickness of oxide layer. The oxide layer thicknesses formed after 24 h oxidation were approximately 5, 12.5 and 50 μm for oxidation at 500, 550 and 600° C, respectively.

TABLE III Parabolic rate constants for the oxidation of Type 1 alloy in the temperature range from 650 to 950° C

Temperature (° C)	Rate constant (g^2 cm^{-4} sec^{-1})		
	K_{pi}	K_{pm}	K_{pf}
650	3.56×10^{-10} (< 8 h)	–	6.30×10^{-11} (> 8 h)
700	2.12×10^{-10} (< 4 h)	–	3.96×10^{-11} (> 4 h)
750	1.46×10^{-10} (< 2 h)	–	6.29×10^{-11} (> 2 h)
800	2.1×10^{-10} (< 3 h)	5.71×10^{-10} (3 to 10 h)	3.64×10^{-10} (> 10 h)
850	3.76×10^{-10} (< 3 h)	9.78×10^{-10} (3 to 13 h)	1.92×10^{-10} (> 13 h)
900	7.05×10^{-10} (< 8 h)	–	6.7×10^{-11} (> 14 h)
950	1.39×10^{-9} (< 5 h)	–	6.54×10^{-11} (> 8 h)

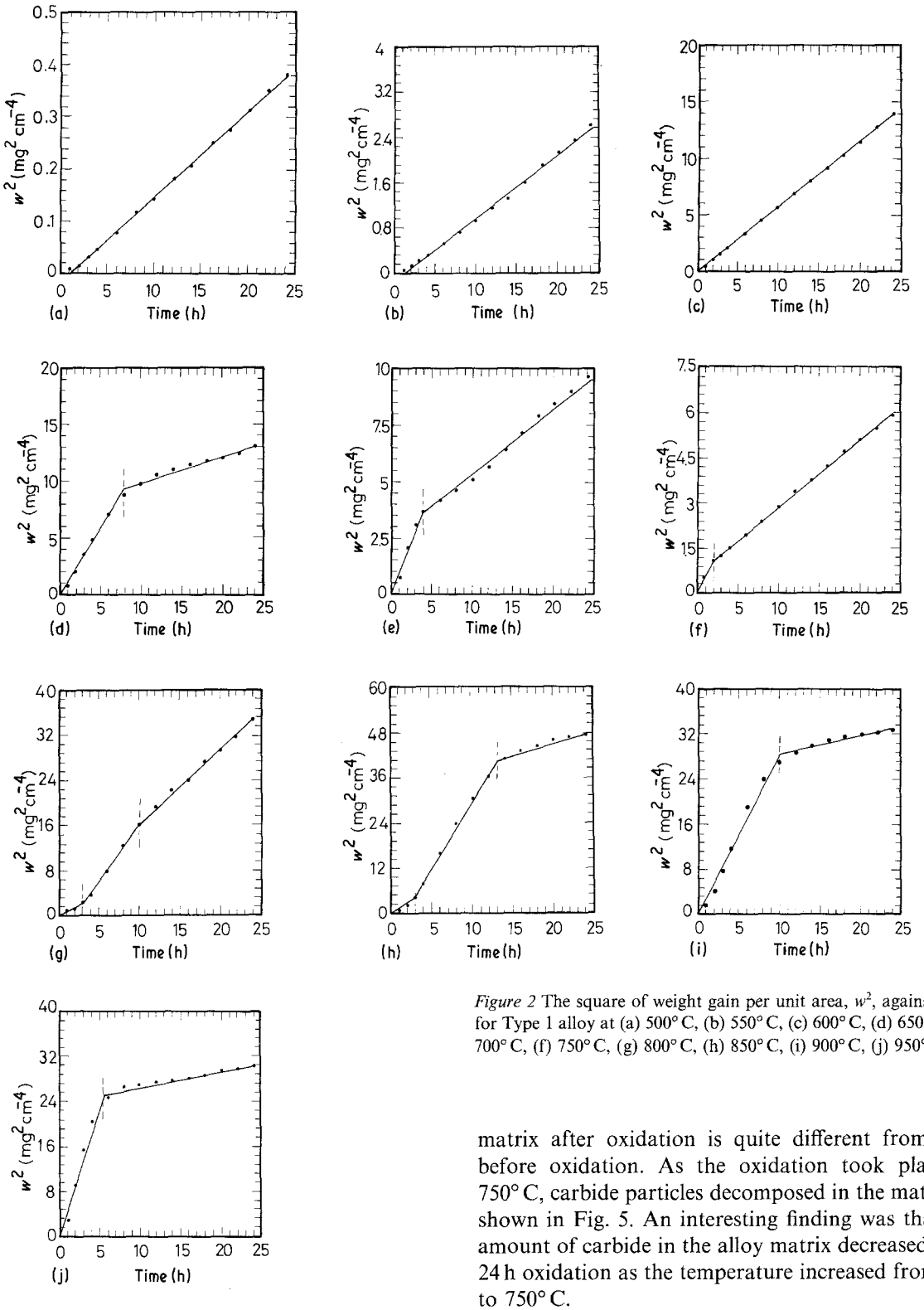

Figure 2 The square of weight gain per unit area, w^2, against time for Type 1 alloy at (a) 500° C, (b) 550° C, (c) 600° C, (d) 650° C, (e) 700° C, (f) 750° C, (g) 800° C, (h) 850° C, (i) 900° C, (j) 950° C.

Fig. 3 shows an optical micrograph of a cross-section of Type 1 alloy after 24 h oxidation at 650° C. The oxide morphologies on the surface of the alloy for oxidation at 650 and 600° C were quite different. At 650° C, the oxide layer grew into the substrate forming a non-planar film. A thin carbide-free layer was observed at the alloy–scale interface of Type 1 alloy. The oxide scales formed after 1 h oxidation at 700° C are shown in Fig. 4. A carbide-free layer can be easily observed along the alloy–scale interface of Type 1 alloy under such conditions. The same result, a carbide-free layer, can also be observed after 24 h oxidation at 750° C. However, the carbide in the alloy matrix after oxidation is quite different from that before oxidation. As the oxidation took place at 750° C, carbide particles decomposed in the matrix as shown in Fig. 5. An interesting finding was that the amount of carbide in the alloy matrix decreased after 24 h oxidation as the temperature increased from 650 to 750° C.

The metallographic cross-sections of Type 1 alloy oxidized for 24 h at from 800 to 950° C indicate the existence of many nodules on the surface. However, no carbide could be observed in the matrix. Figs 6a and b reveal the ellipsoidal shape of the nodules on the surface of the alloy after 24 h oxidation at 850 and 950° C. According to electron microprobe analysis, the upper half of a nodule is rich in iron, but has negligible aluminium. The lower region has a high aluminium concentration of about 8 wt %. In addition, the aluminium concentration increases to a value of about 18 wt % close to the alloy–oxide interface. No carbide could be found in the matrix after 24 h oxidation at from 800 to 950° C.

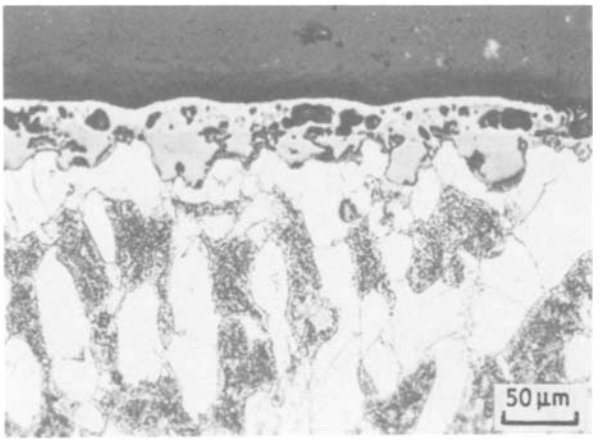

Figure 3 Metallographic cross-section of the oxide scale on Type 1 alloy after 24 h at 650° C.

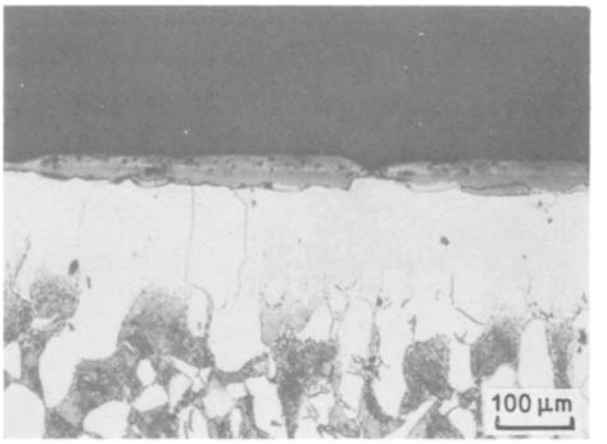

Figure 4 Metallographic cross-section of the oxide scale on Type 1 alloy after 1 h at 700° C.

Fig. 7 shows the kinetic curves for Type 2 alloy at different experimental temperatures. The oxidation rate increased with temperature to a maximum at about 600° C and then decreased to a minimum at about 800° C. According to the square of weight gain against time curves for this alloy, the oxidation behaviour in the temperature range from 500 to 900° C follows two parabolic rate laws for up to 24 h. The parabolic rate constants of the Type 2 alloy oxidation at 500 to 900° C during 24 h were calculated and are listed in Table IV. These results are quite similar to those of previous reports for Fe–Al alloys [2–4]. It is suggested that the effect of temperature on the oxidation of the present alloy under such conditions is due to the preferential oxidation of aluminium at high temperatures. The increase in oxidation rate with increasing temperature up to 600° C is probably associated with a temperature-dependent increase in iron ion diffusion rate through the hercynite layer. Above 600° C the reaction producing aluminium oxide began to predominate. Initially the iron oxide and hercynite were formed on the surface as well, when there was insufficient aluminium in the surface layer to form a complete alumina film. Subsequently aluminium atoms diffused to the oxide–metal interface and formed additional alumina by displacement reactions with $FeAl_2O_4$ and iron oxides. Thus, as temperature was increased, the mobility of aluminium atoms in the alloy increased, more and more protective aluminium oxide was formed, less and less iron oxide and hercynite remained, and the overall oxidation rate dropped.

Webb *et al.* [5] have presented a general discussion of the oxidation of metal–carbon alloys. They discussed two general reaction sequences: (i) diffusion of carbon to the metal–scale interface, where it reacts with the scale to produce gaseous carbon oxides which may accumulate and cause rupture of the scales, and (ii) diffusion of carbon through the scale to react with oxygen at the scale–gas interface. The second sequence would allow decarburization to take place without scale rupture. Bohnenkamp and Engell [6] oxidized Fe–C alloys in air and in CO–CO_2 mixtures over the temperature range 750 to 1050° C and found that the specimens oxidized in air decarburized without scale rupture. Bohnenkamp and Engell proposed that pores present in the scales on Fe–C alloys permitted the diffusion of the carbon oxides. From the present investigation, it was observed that the oxidation behaviours for the Fe–5.5Al–0.55C alloy after two types of heat treatment were quite different. The carbide particles in the matrix of Type 1 alloys are stable at 500, 550 and 600° C, but the oxidation resistance of Type 1 alloy is lower than that of Type 2 alloy under such conditions (Tables III and IV). It is suggested that dissociation of these carbides occurs only

TABLE IV Parabolic rate constants for the oxidation of Type 2 alloy in the temperature range from 500 to 900° C

Temperature (° C)	Rate constant ($g^2 cm^{-4} sec^{-1}$)	
	K_{pi}	K_{pf}
500	5×10^{-12} (< 9 h)	2.5×10^{-12} (> 9 h)
600	4×10^{-11} (< 8 h)	4.4×10^{-12} (> 12 h)
700	4.5×10^{-12} (< 9 h)	3.3×10^{-12} (> 9 h)
800	3×10^{-13} (< 6 h)	1.8×10^{-13} (> 6 h)
900	4×10^{-12} (< 4 h)	1.3×10^{-12} (> 4 h)

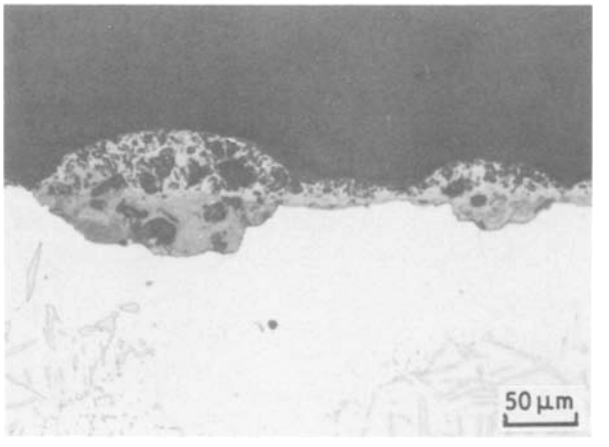

Figure 5 Metallographic cross-section of the oxide scale on Type 1 alloy after 24 h at 750° C.

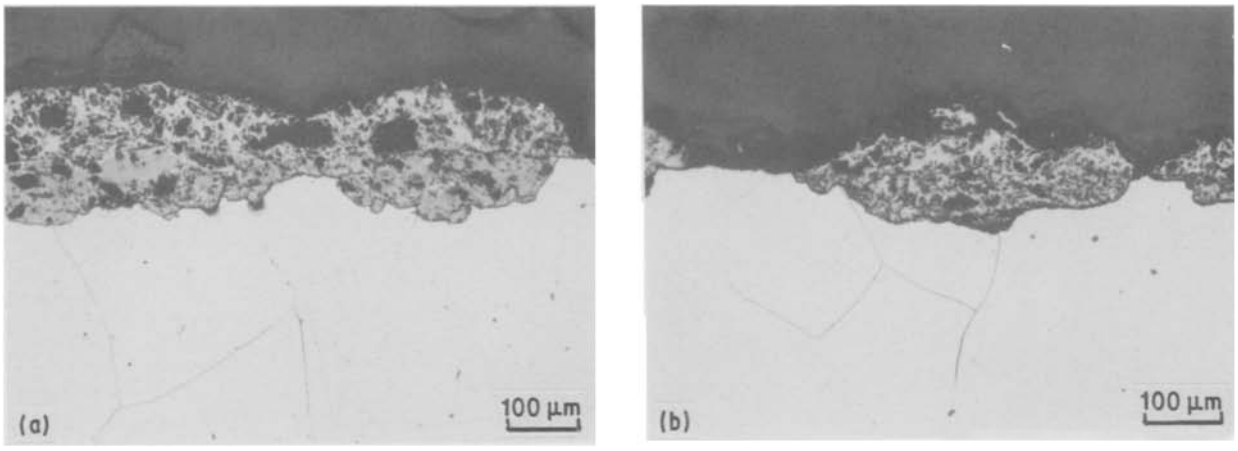

Figure 6 Metallographic cross-section of nodules on Type 1 alloy after 24 h at (a) 850° C, (b) 950° C.

as carbide contacts the atmosphere or touches the oxide scales of the Type 1 alloy. Therefore, no carbide-free region could be formed along the interface between the oxide and matrix at low temperatures. The influence of carbon on the oxidation behaviour is closely related to the decomposition of the carbide near the oxide–matrix interface. Evolution of CO or CO_2 gas always leaves holes in the oxide scale which provide rapid diffusion paths for oxygen and/or iron ions and apparently interfere with the protective spinel or alumina oxide. Thus, the oxidation rate of Type 1 alloy is higher than that of Type 2 alloy under such conditions. The activation energy of 47.7 kcal mol^{-1} (199.7 kJ mol^{-1}) oxidation from 500 to 600° C is quite similar to that reported by Channing and Graham [7] for iron oxide formed on iron at 450 to 550° C with the activation energy 49 kcal mol^{-1}. Therefore, oxidation of the present alloy seems to be mainly controlled by the diffusion of iron ions through the iron oxide. We have recently reported [1] the oxide growth mechanism for Type 1 alloy after oxidation at 600° C.

According to kinetic studies, the initial oxidation rates (K_{pi}) of Type 1 alloy at 650 to 750° C are observed to have about the same order of magnitude oxidation rate (K_p) as at 600° C. Such a similarity can be explained because the alloy has a comparably lower dissociation rate of carbide particles and lower diffusion rate of carbon atoms in this temperature range (Figs 4, 5 and 6). However, the final oxidation rates (K_{pf}) in this temperature range are lower than the oxidation rate (K_p) at 600° C. Thus, the final weight gains of the alloy after 24 h oxidation at 650 to 750° C are lower than that at 600° C. The most reasonable explanation for this is that the diffusion rate of aluminium in such a temperature range of 650 to 750° C was higher than that at 500 to 600° C in the present alloy, which induces the aggregation of aluminium atoms and the formation of an aluminium oxide layer. The results of the present study were confirmed by the EPMA technique, which indicated an inner oxide layer with a relatively high aluminium content after 24 h oxidation at 650 to 750° C. The initial and final oxidation behaviours of Type 1 alloy in the temperature range from 650 to 750° C are apparently controlled by the diffusion of iron ions through the iron oxide and inner aluminium oxide layers, respectively. Similar oxidation behaviours are also observed for Type 2 alloy (Fig. 7). Similar results for Fe–Al oxidation have been reported by Boggs [3].

Based on the square of weight gain against time curves, Type 1 alloy after oxidation at 800 and 850° C can be divided into three stages during 24 h (Figs 2g and h). The deviation of the slope where the oxidation behaviour changes from the first stage to the second stage is related to the evolution of CO or CO_2 along the oxide–alloy interface and is the main factor resulting in the rupture of the oxide layer and, in turn, changing the kinetics of the oxidation process. As the oxidation at 800 or 850° C proceeds, carbon atoms from the decomposition of carbide particles diffuse out to the specimen surface and evaporated with the formation of CO or CO_2. The carbon concentration in the matrix is therefore decreased as oxidation proceeds. When the carbon content is lower than a certain level, evolution of CO (or CO_2) gas can be restricted, which leads to the starting of the third stage of oxidation, a stage with a lower oxidation rate than the second stage of oxidation. The previous discussion is confirmed by Table V, which shows the thickness of the decarburization layer for the oxidation of

TABLE V Thickness of the decarburization layer for the oxidation of Fe–5.5Al–0.55C alloy (heat treatment of Type 1) at 800° C for different experimental times

Time (h)	1	2	4	> 10
Thickness (μm)	112.5	185 to 215	375 to 425	Full decarburization

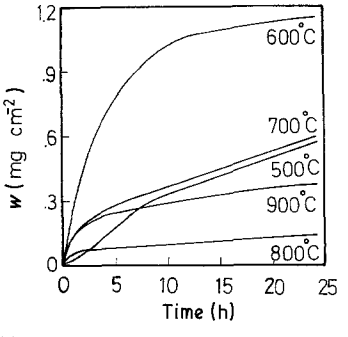

Figure 7 The kinetic curves for Type 2 alloy at different temperatures.

Fe–5.5Al–0.55C alloy (heat treatment of Type 1) at 800° C for different experimental times. The phenomenon of a decarburized zone below the oxide–alloy interface occurs when the rate of diffusion of carbon in the alloy exceeds the rate of diffusion of iron ions into the scale at a given temperature [8]. Similar results are also reported by Boggs [3] and Webb *et al.* [5]. They concluded that carbon from the substrate can react with iron oxides to produce high-pressure CO (or CO_2) pockets which burst through the film and allow oxygen to reach the substrate, promoting the nodular oxide. The high weight gain of the oxidized specimen after 24 h oxidation at 800 and 850° C mainly results from the formation of such nodules.

According to the kinetic curves obtained at 900 and 950° C, there are two distinct parabolic rates for the Type 1 and 2 alloys. Although the oxidation behaviours of Type 1 alloy at 900 and 950° C are similar to those for oxidation at 650 to 750° C, the effect of carbon on the oxidation, judged by optical investigations, is different. Kinetic studies combined with morphology investigations on Type 1 alloy demonstrated that the largest portion of the oxide scales was occupied by iron oxide nodules. Boggs [3] suggested that there appear to be two ways that carbon can interfere with the protective alumina and allow nodular iron oxide to nucleate. The direct oxidation of carbon at random sites in competition with iron and aluminium might leave holes in the film at which nodules might nucleate. Alternatively, carbon from the substrate can react with iron oxides in the initial film to produce high-pressure CO pockets which burst through the film and allow oxygen to reach the substrate, nucleating the nodular oxide. A similar mechanism may account for the increase in the oxidation rate of Type 1 alloy at 900 to 950° C. The dissociation of carbide particles and the diffusion rates of carbon and iron in the alloy at 900 and 950° C are higher than those of the alloys at 500 to 850° C. Thus the initial oxidation rates of the alloy at 900 and 950° C are higher than those at 500 to 850° C. As the carbide particles are totally dissociated and most of the carbon is lost through the pores and microcracks, then the second oxidation rate starts.

It is very interesting to note that no carbide can be found in the matrix of the third stage of oxidation at 800 to 850° C and the second stage of oxidation at 900 to 950° C for Type 1 alloy, which has a higher oxidation rate than Type 2 alloy under same conditions (Figs 1 and 8). A possible reason can be suggested as follows. As the third stage of the oxidation at 800 to 850° C and the second stage of the oxidation at 900 to 950° C occur for Type 1 alloy, the carbon content is lower than a certain level and evolution of CO or CO_2 gas can be restricted, which always might leave holes in the film and support rapid diffusion channels for oxygen and/or iron ions. On the other hand, the Fe–5.5Al–0.55C alloy after Type 2 heat treatment can be considered as an Fe–Al alloy only and the effect of carbon on the oxidation of the alloy can be neglected. Under such conditions the behaviour of Type 2 alloy is due only to the preferential oxidation of aluminium. Thus the oxidation rates of the third stage of oxidation at 800 to 850° C and the second stage of oxidation at 900 to 950° C for Type 1 alloy are higher than for Type 2 alloy.

4. Conclusions

1. Before oxidation, the Fe–5.5Al–0.55C alloy after hot forging and 4 h homogenization at 1100° C under an argon protective atmosphere, referred to as Type 1 alloy, was found to be a two-phase material with iron–aluminium carbide in the ferrite matrix. Type 2 alloy, the present alloy after forging and 96 h homogenization at 1100° C under an air atmosphere, had no carbides and only ferrite in the matrix.

2. The oxidation kinetics of Type 1 alloy after 24 h oxidation at 500 to 950° C can be classified into four groups. The differences in oxidation behaviour among those four groups are controlled by the stability of carbide particles and the diffusion rate of all elements (carbon, aluminium and iron) at different oxidation temperatures from 500 to 950° C. The carbon atoms which come from the dissociation of carbide particles in the matrix play a most important role in the oxidation behaviour in this temperature range. The interference of CO or CO_2 formation influences vitally the formation of protective aluminium oxide.

3. During the oxidation of Type 2 alloy at 500 to 900° C with 24 h, two oxidation periods appear with slightly different parabolic constant values. The oxidation rate increases with temperature to a maximum at about 600° C and then decreases to a minimum at about 800° C. Under these conditions, the oxidation behaviour of Type 2 alloy is due only to the preferential oxidation of aluminium at different temperatures.

4. The oxidation rate of Type 1 alloy with or without a decarburized zone after oxidation is always higher than that of Type 2 alloy.

Acknowledgement

The authors are pleased to acknowledge the financial support of this research by National Science Council, Republic of China under Grant N.S.C. 75-0201-E007-03.

References

1. C. H. KAO and C. M. WAN, *J. Mater. Sci.* **23** (1988) 744.
2. F. SAEGUSA and L. LEE, *Corrosion* **22** (1966) 168.
3. W. E. BOGGS, *J. Electrochem. Soc.* **118** (1971) 906.
4. P. R. S. JACKSON and G. R. WALLWORK, *Oxidat. Met.* **21** (1984) 135.
5. W. W. WEBB, J. T. NORTON and C. WAGNER, *J. Electrochem. Soc.* **103** (1956) 112.
6. K. BOHNENKAMP and H. J. ENGELL, *Arch. Eisenhüttenw.* **33** (1962) 359.
7. D. A. CHANNING and M. J. GRAHAM, *Corros. Sci.* **12** (1972) 271.
8. W. E. BOGGS and R. H. KACHIK, *J. Electrochem. Soc.* **116** (1969) 424.

Received 9 April
and accepted 29 May 1987